

## Preparation of Amphiphilic Magnetic Nanoparticle Suspension via Site-Exchange Reaction

Daisuke Aoki,<sup>1</sup> Kaori Kamata,<sup>1,2</sup> and Tomokazu Iyoda<sup>1,2\*</sup>

<sup>1</sup> Division of Integrated Molecular Engineering, Chem. Res. Lab., Tokyo Institute of Technology

4259 Nagatsuta-Cho, Midori-Ku, Yokohama, Kanagawa 226-8503, Japan

<sup>2</sup> CREST-JST, 4-1-8 Honmachi, Kawaguchi, Saitama 332-0012, Japan

Fax: +81-45-924-5247, e-mail: iyoda@res.titech.ac.jp

**Abstract** Amphiphilic superparamagnetic iron oxide nanoparticles ( $\gamma\text{-Fe}_2\text{O}_3$ ) were synthesized by site-exchanging hydrophobic  $\gamma\text{-Fe}_2\text{O}_3$  nanoparticles soluble in only hydrocarbon solvent such as toluene and hexane with the use of [2-(2-methoxy-ethoxy)-ethoxy]-acetic acid (MEEAA) as exchanging ligands. The reaction conditions were examined with the different time and feeding ratio of MEEAA, leading to the formation of both oil- and water-based magnetic suspensions of  $\gamma\text{-Fe}_2\text{O}_3$  capped with MEEAA. By optimizing the experimental conditions, the amphiphilic spherical particles with size of 5.7 nm were routinely generated in large quantities. UV-vis and FT-IR spectral measurements indicated that the carboxylic end groups of MEEAA were chemically anchored onto the surfaces of  $\gamma\text{-Fe}_2\text{O}_3$  nanoparticles to form stable monolayer coatings. This novel material due to the oligoether mantle around the particle surfaces could function as stable ferrofluids available for various kinds of solution media.

*Key words:* Iron-Oxide nanoparticle, Site-Exchange, Hydrophilic Suspension, Surface Modification

### Introduction

Superparamagnetic iron oxide nanoparticles ( $\gamma\text{-Fe}_2\text{O}_3$ ) have been intensively studied as the most promising candidates for many important technological applications [1] such as refrigeration system [2], color imaging [3], bioprocessing [4], catalysis, drug targeting [5] due to their unique electromagnetic, tribological, and thermomechanical properties. Preparation of magnetic nanoparticles continues to attract a great deal of attention. A variety of chemical and physical preparative methods has been explored to generate nano-sized magnetic fluids with monodisperse size and shape, using thermal decomposition [6], laser pyrolysis [7], reduction of metal salts [8], and electrochemical technique [9]. For instance, one of the recent successes for the synthesis of  $\gamma\text{-Fe}_2\text{O}_3$  nanoparticles has been carried out by two steps: thermal decomposition of iron pentacarbonyl ( $\text{Fe}(\text{CO})_5$ ) in the presence of oleic acid as the stabilizer and oxidation of the formed iron particles with trimethylamine oxide [10]. Since these efforts are conducted by organic ligands with hydrocarbon chains, the nanoparticles obtained are dispersed into most of non-polar organic solvents. The typical technical application, however, requires the magnetic nanoparticles to be sufficiently stable and dispersible in a variety of media, especially, in alcohols or water. Very little work has been done for synthesizing hydrophilic nanoparticles because of the lack of suspension stability. Multilayer coatings have been developed to address the stability of aqueous suspensions. These coating are achieved by ligand-exchange reaction [11] or overcoating of the particles with the other surfactants, polymers, or proteins [12]. The drawbacks of these processes are that they take several steps including syntheses of coating molecules and still have difficulties in avoiding formation of aggregation. Development of high-quality suspension in desired solvent system is still challenge and center of research interests in the field of

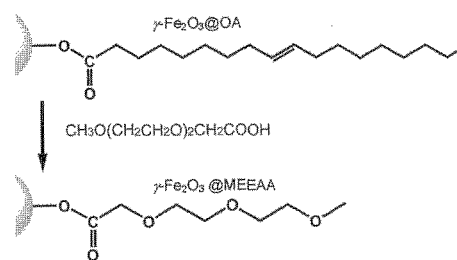


**Figure 1** Schematic drawing of site-exchange reaction from oleic acid (OA) originally capping the surface to [2-(2-methoxy-ethoxy)-ethoxy]-acetic acid (MEEAA).

nanoparticle syntheses.

Here we report a versatile and simple method of site-exchange of particle surface to yield stable suspensions of monodispersed  $\gamma\text{-Fe}_2\text{O}_3$  nanoparticles whose surfaces were protectively and functionally coated with amphiphilic ligand, [2-(2-methoxy-ethoxy)-ethoxy]-acetic acid (MEEAA, Fig. 1). Since this ligand used throughout this study is commercial available, any other treatment is not necessary to examine the surface modification. The resulting site-exchanged particles are easily dissolved into both conventional organic solvents like toluene, chloroform and polar solvents like alcohols and water, allowing the production of amphiphilic magnetic nanoparticle suspensions. The unique properties in conjunction with uniform and ultrafine size of superparamagnetic  $\gamma\text{-Fe}_2\text{O}_3$  nanoparticles could make them valuable for many technological and other applications.

### Experimental

*Chemicals:* All chemicals were of reagent grade and used without further purification. [2-(2-Methoxy-ethoxy)-ethoxy]-acetic acid (MEEAA)

was purchased from Aldrich.

#### Synthesis of amphiphilic $\gamma\text{-Fe}_2\text{O}_3$ nanoparticles:

$\gamma\text{-Fe}_2\text{O}_3$  nanoparticles coated with oleic acid (OA) were synthesized by thermal decomposition of  $\text{Fe}(\text{CO})_5$ , according to the method developed by Hyeon et al. [10] The resulting nanoparticles easily formed aggregations by adding ethanol and, successively, were separated from the solution by centrifugation. The collected aggregates were redispersed in chloroform. This cycle of separation and redispersion was repeated several times to remove the free OA, producing the purified OA-capped nanoparticle ( $\gamma\text{-Fe}_2\text{O}_3\text{@OA}$ ) suspension. For site-exchange reaction, MEEAA chloroform solution was added to the chloroform suspension. Details of the reaction conditions were listed in Table 1.  $\gamma\text{-Fe}_2\text{O}_3\text{@OA}$  nanoparticles of 15 mg and 5 mg were used for preparation of 5 mL chloroform suspensions in Run 1–8 and Run 9–15, respectively. The reaction mixture was sonicated at 50 °C for up to 24 hrs. Small amount of black precipitate was obtained as unreacted nanoparticles upon adding excess ethanol and centrifuging. After removal of the black precipitates, the resulting supernatant generated aggregation of pure  $\gamma\text{-Fe}_2\text{O}_3\text{@MEEAA}$  nanoparticle in diethyl ether. The collected  $\gamma\text{-Fe}_2\text{O}_3\text{@MEEAA}$  was redispersed in ethanol.

**Characterization:** Surface coverage of MEEAA was estimated in the following manner. After removing the excess amount of MEEAA with diethyl ether, 3.8 mg of  $\gamma\text{-Fe}_2\text{O}_3\text{@MEEAA}$  nanoparticles was decomposed with HCl. The  $\text{Fe}^{3+}$  was removed as iron sulfide by adding  $\text{Na}_2\text{S}$  under basic condition. The filtrate was neutralized and then completely evaporated to analyze the amount of MEEAA in the residue by  $^1\text{H-NMR}$  with dioxane as internal standard. The surface coverage was calculated by assuming 25 Å<sup>2</sup> of an occupied area of MEEAA on the particle surface [13]. Particle morphology was studied by transmission electron microscopy (TEM), employing a HITACH-7100 with an acceleration voltage of 100 kV. For TEM sample, small portion of nanoparticle suspensions was placed directly onto the carbon-coated copper grids. The Fourier transform infrared (FT-IR) spectra were recorded by JASCO FT/IR 660 plus spectrometer using KBr pellets. The stabilities of particle suspensions were evaluated by monitoring the characteristic absorption of the suspension with a SHIMADZU MPC-3100 UV-vis spectrometer. As the sample preparations,  $\gamma\text{-Fe}_2\text{O}_3\text{@OA}$  and  $\gamma\text{-Fe}_2\text{O}_3\text{@MEEAA}$  nanoparticles precipitated by ethanol and diethyl ether, respectively, were redispersed in toluene, ethanol, and water to evaluate the suspension stabilities.

#### Result and Discussion

Highly monodispersed  $\gamma\text{-Fe}_2\text{O}_3$  nanoparticles were synthesized by Hyeon method using OA as stabilizer. The XRD profile cannot actually discern between magnetite ( $\text{Fe}_3\text{O}_4$ ) and  $\gamma\text{-Fe}_2\text{O}_3$  (both magnetic oxides have a spinel-type structure), the nature of the ion oxide particles in the final sample was, therefore, analyzed by temperature-dependent Mössbauer spectroscopy. The spectrum displayed full magnetic hyperfine structure and the formation of maghemite particles ( $\gamma\text{-Fe}_2\text{O}_3$ ) was advocated with the characteristic properties such as the values of hyperfine fields and the zero quadrupole

**Table 1** Experimental conditions and amount of sedimentations of unreacted nanoparticles after site-exchange reaction.

Run #*1	Time [h]	MEEAA [mM]	MEEAA/O A	Aaggration*2 [mg]
1	0	0.3	6.7	12 (80 %)
2	0.5	0.3	6.7	15 (100 %)
3	1	0.3	6.7	14 (93 %)
4	2	0.3	6.7	15 (100 %)
5	4	0.3	6.7	11 (73 %)
6	8	0.3	6.7	10 (67 %)
7	12	0.3	6.7	6 (40 %)
8	24	0.3	6.7	3 (20 %)
9	24	0	0	5 (100 %)
10	24	0.03	2	4 (80 %)
11	24	0.06	4	3 (60 %)
12	24	0.2	10	2 (40 %)
13	24	0.3	20	2 (40 %)
14	24	0.6	40	1 (20 %)
15	24	1.2	80	2 (40 %)

(1)  $\gamma\text{-Fe}_2\text{O}_3\text{@OA}$  nanoparticles of 15 mg and 5 mg were used in Run 1–8 and Run 9–15, respectively, for preparing 5 mL of suspensions.

(2) Amount of sedimented aggregates in ethanol consisting of unreacted nanoparticle. Parenthesis shows yield of aggregates obtained by total weight of nanoparticles in initial stage.

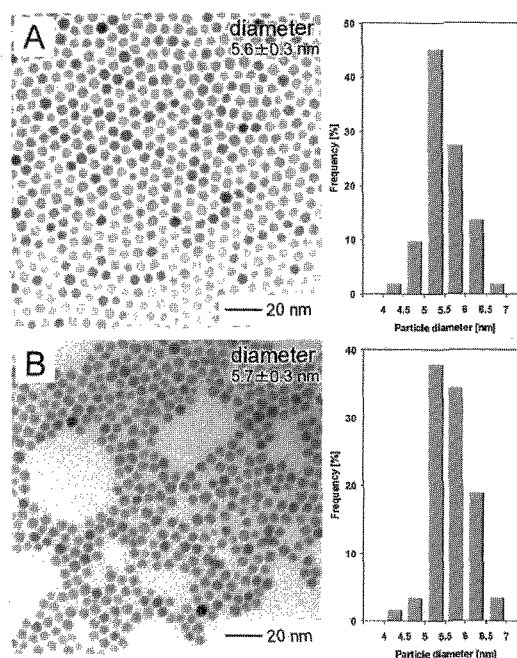


**Figure 2** TEM images of (A)  $\gamma\text{-Fe}_2\text{O}_3\text{@OA}$  nanoparticles and (B)  $\gamma\text{-Fe}_2\text{O}_3\text{@MEEAA}$  nanoparticles obtained after site-exchange reaction and their particle size distributions.

splitting.

Since the  $\gamma\text{-Fe}_2\text{O}_3\text{@OA}$  nanoparticle surface was hydrophobic, the suspensions in hydrocarbon solvent was only stably prepared, indicating formation of sedimented aggregates in polar solvents. Various experimental conditions were adopted to examine site-exchange reactions of  $\gamma\text{-Fe}_2\text{O}_3\text{@OA}$  nanoparticle surfaces, using MEEAA amphiphilic ligand (Table 1). The MEEAA chloroform solutions were added to the as-prepared chloroform suspensions with different molar ratios of MEEAA to OA ( $[\text{MEEAA}]/[\text{OA}]$ ) and then the mixed chloroform solutions were sonicated for up to 24 hrs. The exchange reaction of OA originally capping the nanoparticle surface with MEEAA as the second ligand was supposed as shown in Figure 1. After the

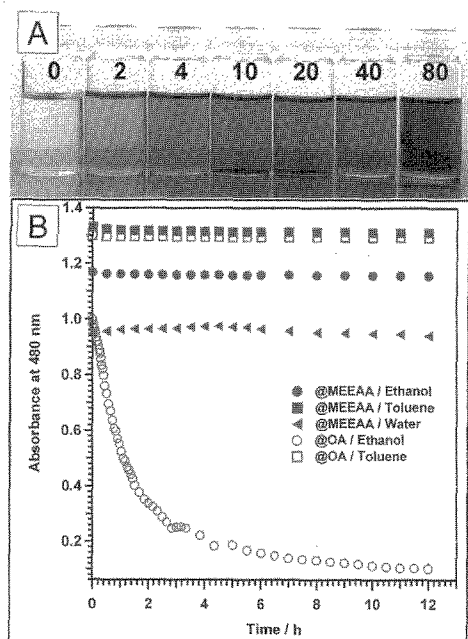


**Figure 3** (A) Stabilities of  $\gamma\text{-Fe}_2\text{O}_3\text{@MEEAA}$  nanoparticle suspensions prepared at the different reaction condition of  $[\text{MEEAA}]/[\text{OA}]$  as insets indicate. (B) Change of optical absorbance at 480 nm as a function of time, evaluating the stabilities of the  $\gamma\text{-Fe}_2\text{O}_3\text{@OA}$  and  $\gamma\text{-Fe}_2\text{O}_3\text{@MEEAA}$  suspensions in the different solvents.

purification with centrifuging/dispersion cycle, solubilities of the resulting nanoparticles against ethanol were estimated by weight of aggregates sedimented upon adding ethanol. A series of oligoethers can be generally dissolved into most of solvent, regardless of hydrophobic or hydrophilic characters, so that oligoether-based molecule has been called as amphiphile. As an evidence of this character, in our present experiments, the highly stable suspensions were still observed in chloroform during the site-exchange treatments. Therefore, the amount of aggregates insoluble in ethanol represented directly that of unreacted particles, which was able to evaluate the efficiency of the site-exchange reaction as a function of the reaction time and  $[\text{MEEAA}]/[\text{OA}]$ . Under the condition of  $[\text{MEEAA}]/[\text{OA}] = 6.7$ , the yield of aggregates consisting of unreacted nanoparticles was decreased from 100 % to 20 % as a function of the reaction time up to 24 hrs. Further sonications did not influence on the amount of aggregates, so that the

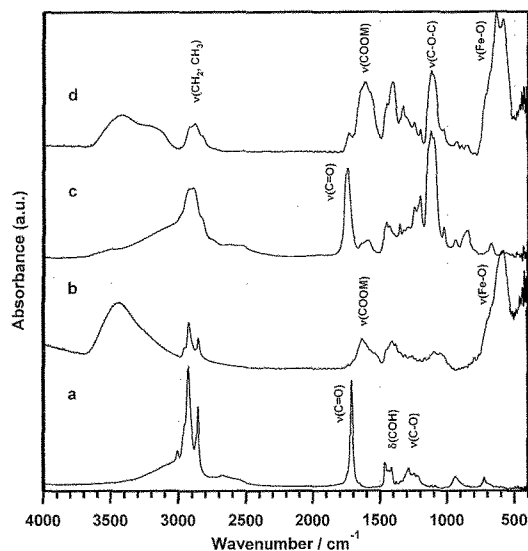


**Figure 4** FT-IR spectra of (a) free OA, (b)  $\gamma\text{-Fe}_2\text{O}_3\text{@OA}$  nanoparticles, (c) free MEEAA, and (d)  $\gamma\text{-Fe}_2\text{O}_3\text{@MEEAA}$  nanoparticles, taken from their KBr pellets.

reaction was completed for 24 hrs. The effect of  $[\text{MEEAA}]/[\text{OA}]$  on the yield as well as quality of the suspension was performed at the different conditions:  $[\text{MEEAA}]/[\text{OA}] = 0, 2, 4, 10, 20, 40, 80$ . High conversion of the site-exchange was demonstrated in above 10 of  $[\text{MEEAA}]/[\text{OA}]$ . The amount of MEEAA released by HCl decomposition in 3.8 mg of  $\gamma\text{-Fe}_2\text{O}_3\text{@MEEAA}$  was  $0.37 \times 10^{-5}$  mol, indicating 67 % of surface coverage. No peak corresponding to OA was detected. Figure 2 shows TEM images and size distributions of  $\gamma\text{-Fe}_2\text{O}_3$  nanoparticles before and after the site-exchange. The  $\gamma\text{-Fe}_2\text{O}_3\text{@OA}$  particles had spherical shape with diameter of 5.6 nm. This structural feature was completely preserved after exchanging the ligands from OA to MEEAA. The monodisperse  $\gamma\text{-Fe}_2\text{O}_3\text{@MEEAA}$  nanoparticles of 5.7 nm diameter were arranged into two-dimensional hexagonal closed packed structure, indicating the uniformity of the spherical particle size.

All of the samples showed dark red-brown color as characteristics in  $\gamma\text{-Fe}_2\text{O}_3$  suspensions. The snapshots of samples dispersed in ethanol depicted high quality of the suspensions and also the reaction efficiency at the different reaction conditions of  $[\text{MEEAA}]/[\text{OA}]$  (Fig. 3A). The dried powders of  $\gamma\text{-Fe}_2\text{O}_3\text{@MEEAA}$  nanoparticles were redispersed in

**Table 2** Assignment of selected absorption bands of OA and MEEAA and the corresponding  $\gamma\text{-Fe}_2\text{O}_3$  nanoparticles.

group vibrations	assignment	symbol	Oleic acid	$\text{Fe}_2\text{O}_3\text{@oleic acid}$	MEEAA	$\text{Fe}_2\text{O}_3\text{@MEEAA}$
methyl	antisymmetric stretching	$\nu_{\text{as}}(\text{CH}_3)$	2956	2952	2990	2986
	symmetric stretching	$\nu_{\text{s}}(\text{CH}_3)$	2872	2868	2889	2881
	scissoring/bending	$\delta(\text{CH}_3)$	1465	1456	1455	1453
methylene	antisymmetric stretching	$\nu_{\text{as}}(\text{CH}_2)$	2925	2922	2928	2922
	symmetric stretching	$\nu_{\text{s}}(\text{CH}_2)$	2854	2852	2832	2826
	scissoring/bending	$\delta(\text{CH}_2)$	1465	1456	1455	1454
	rocking	$\gamma(\text{CH}_2)$	723	overlapped	674	overlapped
carboxylic acid	C=O stretching	$\nu(\text{C}=\text{O})$	1711	1633, 1410	1744	1616, 1405
	C-O-H in-plane bending	$\delta(\text{COH})$	1411	-	1434	-
	C-O stretching	$\nu(\text{C}-\text{O})$	1285	1098	1247	1247, 1030
	O-H scissoring/bending	$\delta(\text{OH})$	937	-	937	-
ether	C-O-C antisymmetric stretching	$\nu_{\text{as}}(\text{C}-\text{O}-\text{C})$	-	-	1121	1120
	C-O-C symmetric stretching	$\nu_{\text{s}}(\text{C}-\text{O}-\text{C})$	-	-	848	-

both non-polar hydrocarbon solvents and polar solvents without addition of any other surfactants. The stabilities of the  $\gamma$ -Fe<sub>2</sub>O<sub>3</sub> nanoparticle suspensions in the different kinds of solvents were evaluated before and after the site-exchange by UV-vis absorption spectral measurements (Fig. 3B). The time-dependent variation of their characteristic optical absorbance at 480 nm was monitored. When the suspensions become unstable, the resulting particle aggregates precipitated and the suspension was diluted to decrease absorbance at 480 nm. The absorbance of  $\gamma$ -Fe<sub>2</sub>O<sub>3</sub>@OA ethanol suspension was rapidly decreased within 2 hrs, while that of toluene suspension kept constant. In contrast, the overall trend of absorbance decrease as a function of time was remarkably restrained in the case of  $\gamma$ -Fe<sub>2</sub>O<sub>3</sub>@MEEAA nanoparticles in all of toluene, ethanol, and water for 2 weeks. Especially, the ethanol suspension was stable over 5 months. It is worthwhile mentioning that MEEAA can function as high performance stabilizer of metal-oxide nanoparticle surface to prepare their suspensions dispersed in both non-polar and polar solvents.

Since there are large surface-to-volume atomic ratio, high surface activity, and amount of dangling bonds on nanoparticle surface, the atoms on the surface are apt to adsorb ions or molecules in solution. For iron-oxide nanoparticles dispersed in solution of acetic acid ended ligands, the bare atoms of Fe and O on the particle surface can react with the ligand and form chemical bonding, Fe-O-C(=O), as illustrated in Figure 1. The fact was proven by comparison of FT-IR spectra of the nanoparticles before and after the site-exchange reactions. The vibration modes characterized the ligands chemically bonded to the  $\gamma$ -Fe<sub>2</sub>O<sub>3</sub> nanoparticle surface (Fig. 4). The selected band assignments of the nanoparticles are given in Table 2. The  $\gamma$ -Fe<sub>2</sub>O<sub>3</sub>@OA nanoparticles showed absorption bands in three characteristic regions: (i) between 2800 and 3000 cm<sup>-1</sup>, associated with vibrations of the -CH<sub>3</sub> and -CH<sub>2</sub> groups in the aliphatic chain, (ii) between 1600 and 1400 cm<sup>-1</sup>, related to the presence of coordinated -COO<sup>-</sup> groups, and (iii) at 600 and 460 cm<sup>-1</sup>, indicative of a rigid  $\gamma$ -Fe<sub>2</sub>O<sub>3</sub> network. After the site-exchange reaction, the bands in the above three regions were essentially unchanged and new absorption band appeared at 1120 cm<sup>-1</sup>, corresponding to stretching vibration of -COC- in the ether units of MEEAA. We perceived a remarkable broadening of the aliphatic absorption bands. The narrowing or broadening CH<sub>2</sub> stretching bands are often used as an indicator for degree of crystallinity of alkyl chain, i.e., immobilization of alkyl chain gives narrow peak width. Therefore, poor crystallinity of the oligoether chain present in  $\gamma$ -Fe<sub>2</sub>O<sub>3</sub>@MEEAA resulted in the broad absorption bands, while the  $\gamma$ -Fe<sub>2</sub>O<sub>3</sub>@OA showed relatively sharp absorption bands due to the highly packed structure of aliphatic chains. The results strongly suggest that the site-exchange of carboxylic units in the parent OA by those of the MEEAA was successfully conducted through the present procedure.

### Conclusion

Stable suspensions of oligoether-capped ultrafine  $\gamma$ -Fe<sub>2</sub>O<sub>3</sub> nanoparticles ( $\gamma$ -Fe<sub>2</sub>O<sub>3</sub>@MEEAA) with

diameter of 5.7 nm were prepared via site-exchange reaction of hydrophobic nanoparticle surface soluble to hydrocarbon solvents. The reaction was optimized with the different conditions like reaction time and feeding ratio of the exchanging ligand. The  $\gamma$ -Fe<sub>2</sub>O<sub>3</sub>@MEEAA nanoparticle was dispersed in both non-polar solvents such as toluene and chloroform and polar solvents such as alcohols and water. The nanoparticles in ethanol, especially, exhibited stable suspensions with no insoluble aggregates over 5 months. Surface modification of magnetic particles with other ligands, bearing functional groups different from the carboxylic group, will be the subject of a future work for biological and industrial magnetic fluid materials. The amphiphilic magnetic nanoparticles should be promising candidates for the fabrication of more sophisticated nanoscale structures.

**Acknowledgments.** This work has been supported in part by a Grant-in-Aid from the Ministry of Education, Culture, Sports, Science, and Technology (MEXT). K.K. thanks Prof. Younan Xia (Univ. of Wash.) for his useful discussion and help with particle synthesis.

### References

- [1] R. M. Cornell and U. Schwertmann, "The iron oxides", VCH, Weinheim (1996).
- [2] R. D. McMichael, R. D. Shull, L. J. Swartzendruber, L. H. Bennett, and R. E. Watson, *J. Magn. Magn. Mater.*, **111**, 29-33 (1992).
- [3] D. Portet, B. Denizot, E. Rump, J. Lejeune, and P. Jallet, *J. Colloid Interface Sci.*, **238**, 37-42 (2001).
- [4] J. Roger, J. N. Pons, R. Massart, A. Halbreich, and J. C. Bacri, *Euro. Phys. J., Appl. Phys.*, **5**, 321-325 (1999).
- [5] S. P. Bhatnagar and R. E. Rosensweig, *J. Magn. Magn. Mater.*, **149**, 198 (1995).
- [6] K. S. Suslick, M. Fang, and T. Hyeon, *J. Am. Chem. Soc.*, **118**, 11960-11961 (1996).
- [7] S. Veintemillas-Verdaguer, O. Bomati, M. P. Morales, P. E. Di Nunzio, and S. Martelli, *Mater. Lett.*, **57**, 1184-1189 (2003).
- [8] (a)K.-L. Tsai and J. L. Dye, *J. Am. Chem. Soc.*, **113**, 1650-1652 (1991). (b)J.-I. Park and J. Cheon, *J. Am. Chem. Soc.*, **123**, 5743-5746 (2001). (c)S. Sun and C. B. Murray, *J. Appl. Phys.*, **85**, 4325-4330 (1999).
- [9] (a)C. Pascal, J. L. Pascal, and F. Favier, *Chem. Mater.*, **11**, 141-147 (1999). (b)B. Yang, Y. Wu, B. Zong, and Z. Shen, *Nano Lett.*, **2**, 751-754 (2002).
- [10] T. Hyeon, S. S. Lee, J. Park, Y. Chung, and H. B. Na, *J. Am. Chem. Soc.*, **123**, 12798-12801 (2001).
- [11] (a)T. Pellogrino, S. Kudera, T. Liedl, A. M. Javier, L. Manna, and J. Parak, *Small*, **1**, 48-63 (2005). (b)M. Kim, Y. Chen, Y. Liu, and X. Peng, *Adv. Mater.*, **17**, 1429-1432 (2005). (c)R. Hong, N. O. Fischer, T. Emrick, and V. M. Rotello, *Chem. Mater.*, **17**, 4617-4621 (2005).
- [12] (a)M. D. Cuyper and M. Joniau, *Langmuir*, **7**, 647-652 (1991). (b)B. Dubertret, P. Skourides, D. J. Norris, V. Noireaux, A. H. Brivanlou, and A. Libchaber, *Science*, **298**, 1759-1762 (2002). (c)A. Chen, H. Wang, B. Zhao, and X. Li, *Synth. Met.*, **139**, 411-415 (2003).
- [13] An occupied area of 25 Å<sup>2</sup> was adopted as conventional standard aliphatic ligands consisting of long alkyl chain, which forms a close-packed structure.